Two-directional nodal model for silicide nanoparticle growth in thermal plasma processing

M. Shigeta[1], T. Watanabe[2]

[1]*Department of Mechanical Systems and Design, Tohoku University, Sendai, Japan*
[2]*Department of Environmental Chemistry and Engineering, Tokyo Institute of Technology, Yokohama, Japan*

Abstract: A new model, which is more precise but easy-to-use, is developed for analyzing silicide nanoparticle growth in thermal plasma processing. The model successfully reveals the growth mechanism that has not been predicted by any other models. The majority of the produced Ti-Si nanoparticles have a near-stoichiometric composition. On the other hand, the Mo-Si nanoparticles have widely ranging diameters and compositions.

Keywords: Modeling, Thermal plasma, Nanoparticle, Silicide, Numerical Simulation

1. Introduction

Thermal plasma has been expected to be a powerful tool to mass-produce nanoparticles even if the nanoparticles consist of intermetallic compounds such as silicides. However, the particle distribution tends to have a large dispersion in the size and composition. Even though the quantitative estimation is strongly demanded, there have not been any models which precisely express the growth mechanism of silicide nanopartilces in thermal plasma processing. In this study, a new model, which is more precise but easy-to-use, is developed on the basis of our previous model [1] so that the growth mechanism is numerically clarified in detail.

2. Computational condition

Figure 1 schematically depicts a nanoparticle synthesis system aided by an induction thermal plasma (ITP) as a target of this study. The plasma is generated by the radio-frequency electromagnetic field with an input power of 5.0kW and an applied frequency of 4.0MHz. Argon gas is injected as the carrier gas (1.0Sl/min), the plasma supporting gas (3.0Sl/min), and the sheath gas (30.0Sl/min) from the top of the system. Precursory powders of metal and silicon are injected (0.1g/min) with the carrier gas from the injection tube, and then they are vaporized in the high-enthalpy field of the ITP. The initial silicon content in the powders is selected to be 66.7at.%, which is the stoichiometric composition of metal disilicides. Our previous numerical study confirmed that the powders are completely vaporized in the plasma torch [1].

The material vapors are transported with the plasma flow to the nanoparticle growth chamber. Because the temperature drastically decreases in the chamber, the material vapors become supersaturated and homogeneous nucleation starts. Once nuclei are generated, the vapors of the metal and silicon co-condense on the nuclei by heterogeneous condensation. Simultaneously the nanoparticles collide, coagulate, and merge with each other. These three processes play important roles in the growth of nanoparticles. In this study, the region right below the plasma torch is chosen as a computational domain in **Fig.1**. The temperature and the velocity in the computational domain are obtained by the magnetohydrodynamics (MHD) approach [1]. The temperature and the velocity decrease monotonically. The computation is carried out under the axially one-dimensional condition.

3. Model description

The present model offers three major advantages: (a) it can describe any profile of particle size distribution (PSD); (b) it can estimate the size and composition of nanoparticles simultaneously; (c) the model formulation is straightforward and arithmetic.

To formulate the model, several assumptions are introduced: (i) spherical nanoparticles; (ii) negligible inertia

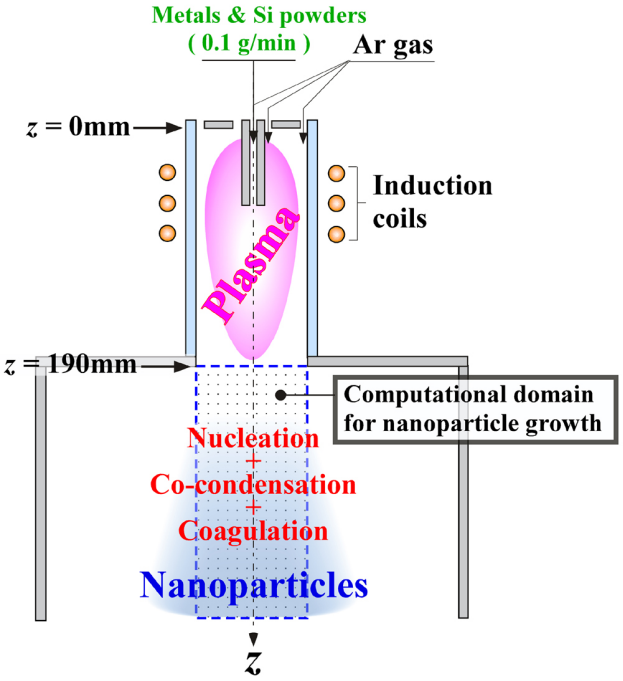

Fig.1 Nanoparticle synthesis system aided by an ITP.

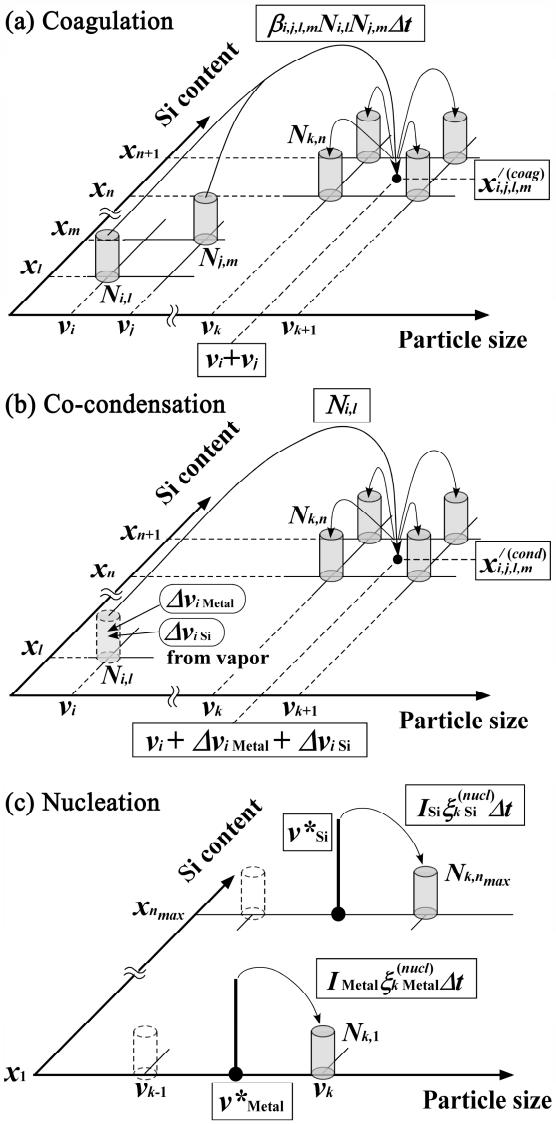

Fig.2 Algorithm of two-directional nodal model.

of nanoparticles; (iii) identical temperature and velocity of nanoparticles to those of the bulk flow; (iv) negligible heat generated by condensation; (v) negligible electric charge of nanoparticles; and (vi) the material vapors regarded as an ideal gas without chemical reactions.

The PSD of a nanoparticle assembly is always given as a function of the particle size. In this study, the PSD is defined as a function of the composition as well as the particle size since the nanoparticles can contain both metal and silicon. Therefore, the particle size-composition distribution (PSCD) is introduced instead of the PSD. PSCD is expressed by nodal discretization for the two individual directions of the particle size and the composition. As shown in **Figs.2(a)** to **2(c)**, the nanoparticles reside only at the nodes.

The nodes are spaced linearly on a logarithmic scale to the size direction; while spaced linearly to the composition direction.

$$v_{k+1} = f_v v_k \quad (k = 1, 2, \dots, k_{max}\text{-}1) \tag{1}$$

$$x_{n+1} = x_n + \Delta x \quad (n = 1, 2, \dots, n_{max}\text{-}1) \tag{2}$$

where v_k is the volume of the particle at node k, and x_n is the fraction of silicon in a particle at node n. In this study, f_v, k_{max}, Δx and n_{max} are set to be 1.6, 58, 0.025 and 41, respectively.

The governing equation for the particle concentration N at the node (k, n) is given by

$$\frac{dN_{k,n}}{dt} = \left[\dot{N}_{k,n}\right]_{coag} + \left[\dot{N}_{k,n}\right]_{cond} + \left[\dot{N}_{k,n}\right]_{nucl} \tag{3}$$

$\left[\dot{N}\right]$ represents the net production rate. The contributions of coagulation, condensation and nucleation are given as

$$\left[\dot{N}_{k,n}\right]_{coag} = \frac{1}{2}\sum_i\sum_j\sum_l\sum_m \xi^{(coag)}_{i,j,k}\psi^{(coag)}_{i,j,l,m,n}\beta_{i,j,l,m}N_{i,l}N_{j,m} - N_{k,n}\sum_i\sum_l \beta_{i,k,l,m}N_{i,l} \tag{4}$$

$$\left[\dot{N}_{k,n}\right]_{cond} = \sum_i\sum_l \frac{(\xi^{(cond)}_{i,k}\psi^{(cond)}_{i,l,n} - \delta_{i,k}\delta_{l,n})N_{i,l}}{\Delta t} \tag{5}$$

$$\left[\dot{N}_{k,n}\right]_{nucl} = I_M \xi^{(nucl)}_{k\ M} \tag{6}$$

ξ and ψ are the splitting operators for the size space and the composition space, respectively. β is the collision frequency function. $\delta_{i,k}$ represents the Kronecker delta. Δt is the time increment. In Eq. (6), n=1 when M=Metal; n=n_{max} when M=Si. I_M is the homogeneous nucleation rate I of material M, which can be estimated by the self-consistent theory [2].

In co-condensation process, the volume increment Δv_{iM} of the particles at the i-th size nodes due to the condensation of material M is accurately calculated by the following equation covering the entire range of Knudsen numbers [3].

$$\frac{\Delta v_{i\,M}}{\Delta t} = 2\pi d_i D_{vapor\,M} v_M (N_{vapor\,M} - N'_{S\,iM}) \times \left[\frac{0.75\alpha_M(1+\mathrm{Kn}_i)}{0.75\alpha_M + 0.283\alpha_M\,\mathrm{Kn}_i + \mathrm{Kn}_i^2}\right] \tag{7}$$

Here, α is the accommodation coefficient. In this study, α is set to be 0.05 which is the reasonable value validated in [4]. D represents the diffusion coefficient. The subscript *vapor* denotes vapor. The concentration in the saturated state N'_S is modified by the Kelvin effect, which is considerable for small particles [5].

The concentrations of the material vapors must be solved simultaneously.

$$\frac{dN_{vapor\,M}}{dt} = \left[\dot{N}_{vapor\,M}\right]_{nucl} + \left[\dot{N}_{vapor\,M}\right]_{cond} \tag{8}$$

$\left[\dot{N}_{vapor\,M}\right]$ represents the net production rate of the vapors of material M.

$$\left[\dot{N}_{vapor\,M}\right]_{nucl} = -\sum_k I_M \xi^{(nucl)}_{kM}\frac{v^*_M}{v_M} \tag{9}$$

$$\left[\dot{N}_{vapor\,M}\right]_{cond} = -\sum_i\sum_l \frac{N_{i,l}\Delta v_{iM}}{v_M \Delta t} \tag{10}$$

v and v^* are the volume of the monomer and the critical volume, respectively.

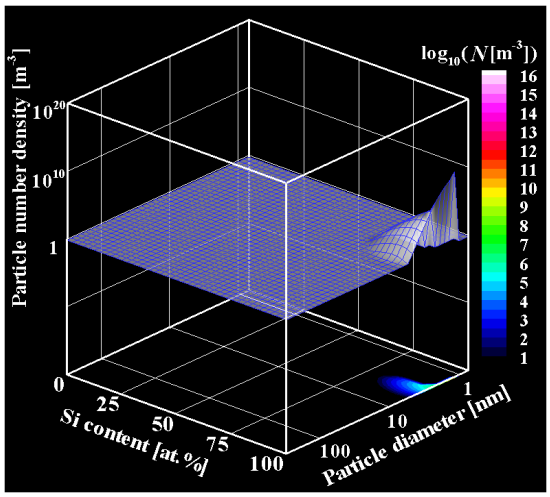

(a) z = 224.50 mm

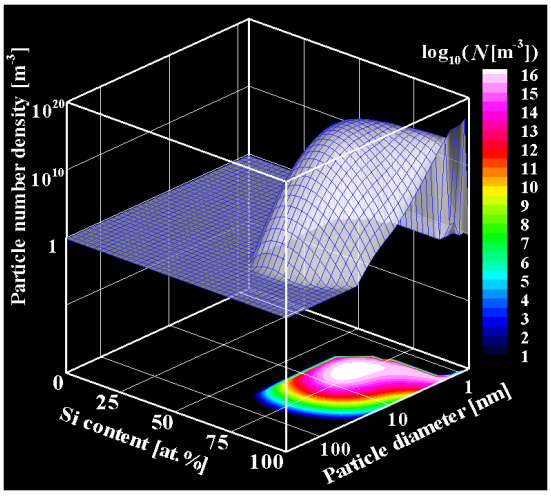

(c) z = 228.00 mm

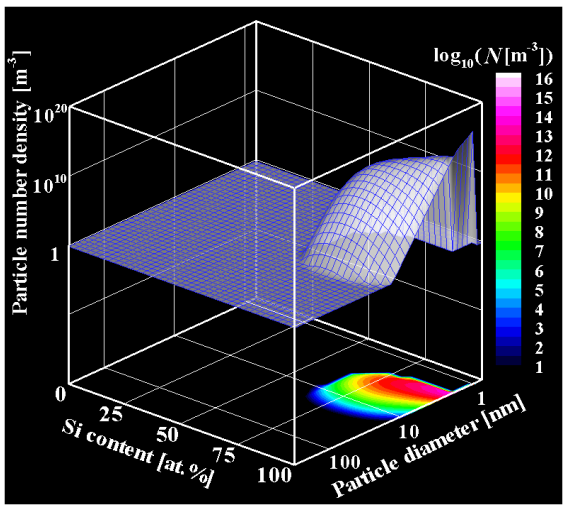

(b) z = 226.00 mm

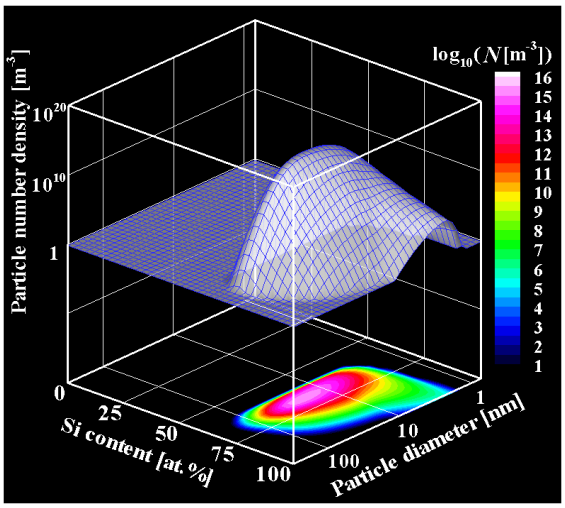

(d) z = 241.00 mm

Fig.3 Nanoparticle growth process for Ti-Si system.

3. Numerical results

Figure 3 shows the nanoparticle growth process in the Ti-Si system. Si vapor first nucleates, and immediately both Si and Ti vapors co-condense on Si nuclei around z = 224.5mm (**Fig.3(a)**). This is because the both vapors reach their supersaturated states simultaneously. Ti-Si nanoparticles rapidly grow up (**Fig.3(b)** and **3(c)**) and finally create their mature profile (**Fig.3(d)**). The majority of the nanoparticles have a near-stoichiometric composition of 60 to 80at.% because of the simultaneous co-condensation of two components. No nanoparticles are produced with an Si content less than 60at.%. However, nanoparticles have widely ranging diameters from a few nanometers to 100nm.

Figure 4 depicts the nanoparticle growth process in the Mo-Si system. In the early stage, pure Mo nanoparticles grow up (**Fig.4(a)**). Through the co-condensation process of Mo and Si vapors (**Fig.4(b)** and **4(c)**), the nanoparticles reach their mature state (**Fig. 4(d)**). Although Mo-Si nanoparticles show a composition range of 15 to 95at.%, most nanoparticles have the diameter around 10nm and the Si content around 66.7%. It is also found that pure Mo nanoparticles around 1nm still remain. This is because smaller particles can gain a smaller amount of vapors due to the rarefied gas effect with larger Knudsen numbers.

Figure 5 presents the comparisons between the results of the present model and those of the experiments [1, 6]. The operating conditions are identical. The numerical results and the experimental results show good quantitative agreements, which endorses the validity of the present model.

4. Summary

A new model, which is more precise but easy-to-use, has been developed and proposed to clarify silicide nanoparticle growth in thermal plasma processing. The model successfully reveals the growth mechanism that has not been predicted by any other models. It can also be concluded that the present model is a useful tool for nu-

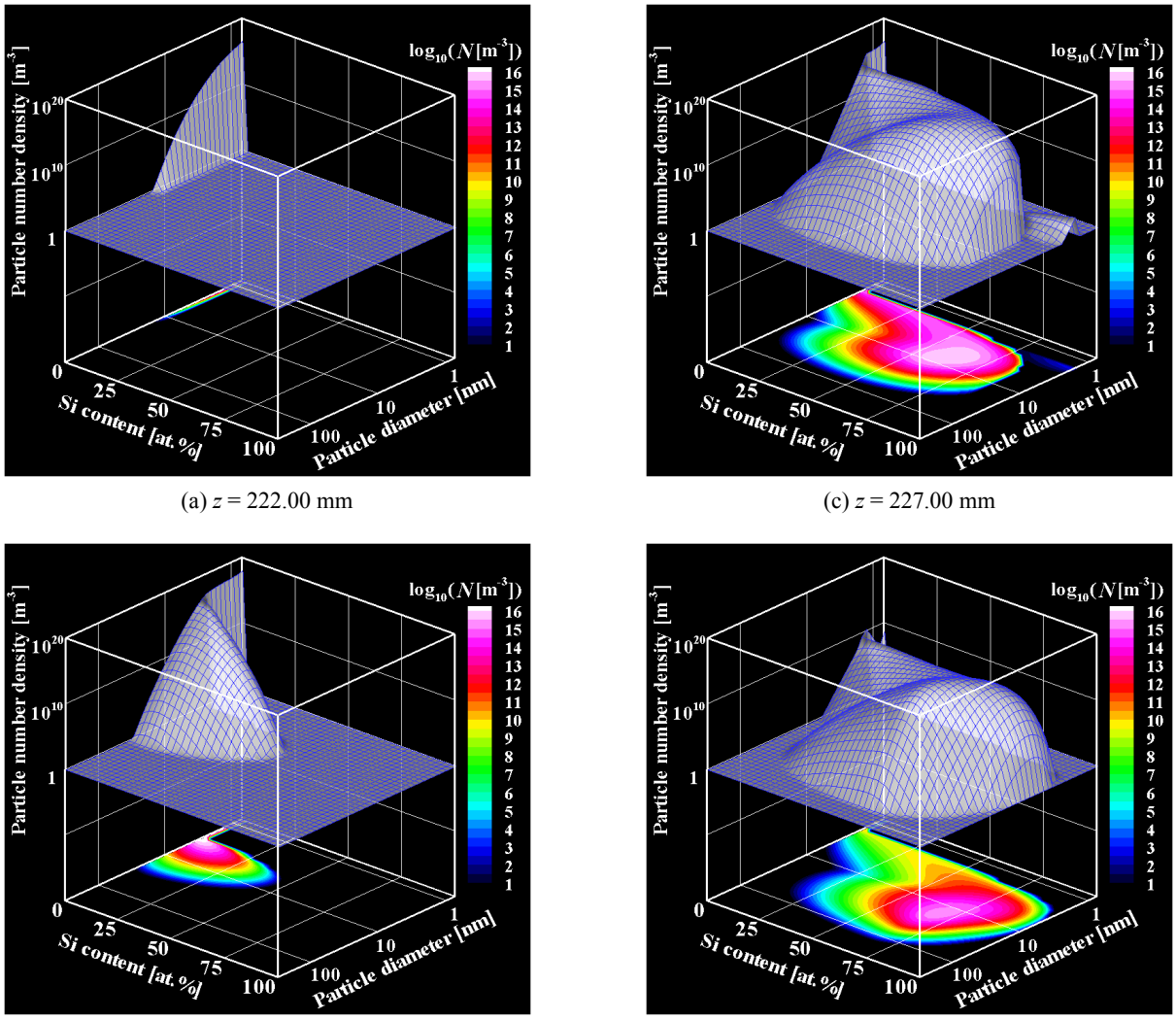

(a) z = 222.00 mm (c) z = 227.00 mm

(b) z = 223.00 mm (d) z = 238.37 mm

Fig.4 Nanoparticle growth process for Mo-Si system.

merically analyzing nanoparticle growth processes, including co-condensation, with sufficient accuracy.

References

[1] M. Shigeta, T. Watanabe, Journal of Physics D: Applied Physics 40, 2407 (2007).

[2] S.L. Girshick, C.-P. Chiu, P.H. McMurry, Aerosol Science and Technology 13, 465 (1990).

[3] J.H. Seinfeld, S.N. Pandis, Atmospheric Chemistry and Physics, From Air Pollution to Climate Change, John Wiley & Sons, Inc., (1998).

[4] M. Shigeta, T. Watanabe, Jounal of Thermal Spray Technology, (2009) in press. (DOI: 10.1007/s11666-009-9316-3)

[5] S.K. Friedlander, Smoke, Dust and Haze, Fundamentals of Aerosol Dynamics 2nd Ed., Oxford University Press, (2000).

[6] T. Watanabe, H. Okumiya, Science and Technology of Advanced Materials 5, 639 (2004).

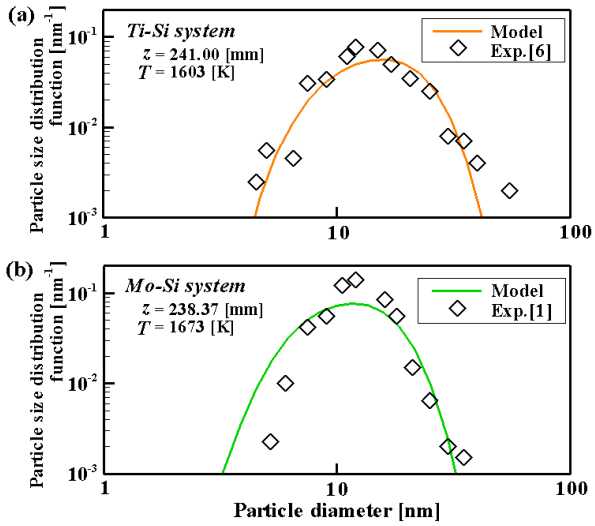

Fig.5 Validation of the present model.